Mitophagy suppression by miquelianin-rich lotus leaves extract induces “beiging” of white fat *via* AMPK/DRP1-PINK1/PARKIN signaling axis

Zhenyu Wang [a,b], Tian Yang [a,b], Maomao Zeng [a,b], Zhaojun Wang [a,b], Qiuming Chen [a,b], Jie Chen [a,b], Mark Christian [*, c], and Zhiyong He [*, a,b]

[a]State Key Laboratory of Food Science and Resources, Jiangnan University, Wuxi, Jiangsu 214122, China

[b]International Joint Laboratory on Food Safety, Jiangnan University, Wuxi, Jiangsu 214122, China

[c]School of Science and Technology, Nottingham Trent University, Clifton, Nottingham, NG11 8NS, United Kingdom

Running Title：Lotus leaves induce beige fat formation in white fat depots

Abstract

Background

Lotus (*Nelumbo nucifera*) leaf has been described to have anti-obesity activity, but the role of white fat "browning" or "beiging" in its beneficial metabolic actions remains unclear. Here, 3T3-L1 cells and high-fat-diet (HFD)-fed mice were used to evaluate the effects of miquelianin-rich lotus leaf extract (LLE) on white-to-beige fat conversion and its regulatory mechanisms.

Results

Treatment with LLE increased mitochondrial abundance, mitochondrial membrane potential, and NAD^+/NADH ratio in 3T3-L1 cells, suggesting its potential in promoting mitochondrial activity. qPCR and/or Western blotting analysis confirmed that LLE induced the expression of beige fat-enriched gene signatures (e.g., Sirt1, Cidea, Dio2, Prdm16, Ucp1, Cd40, Cd137, Cited1) and mitochondrial biogenesis-related markers (e.g., Nrf1, Cox2, Cox7a, Tfam) in 3T3-L1 cells and inguinal white adipose tissue (iWAT) of HFD-fed mice. Furthermore, we found that LLE treatment inhibited mitochondrial fission protein DRP1 and blocked mitophagy markers such as PINK1, PARKIN, BECLIN1, and LC-3B. Chemical inhibition experiments revealed that AMPK/DRP1 signaling was required for LLE-induced beige fat formation *via* suppressing PINK1/PARKIN/mitophagy.

Conclusion

Our data reveal a novel mechanism underlying the anti-obesity effect of LLE, namely the induction of white fat beiging *via* AMPK/DRP1/mitophagy signaling.

Keywords: Lotus leaf extracts, Beige fat, Mitochondrial biogenesis, Mitophagy, AMPK/DRP1

1. Introduction

Obesity occurs as a consequence of energy intake exceeding energy expenditure. In line with the laws of thermodynamics, any treatment for obesity necessarily reduces energy intake, or increases energy expenditure, or has an effect on both.[1] Although restricting calorie intake is the first defense against obesity, metabolic efficiency changes and increased energy expenditure in key metabolic organs (e.g., adipose tissue) are also an important alternative strategy.[2] Adipose tissue is classified into three types based on its origin, functionality, and morphology, namely white, brown, and beige.[3] White adipose tissue (WAT) functions as the major energy storage location, and its main feature is that the adipocytes within it contain individual large lipid droplets and store excess energy as triglycerides, while classical brown adipose tissue (BAT) contains multilocular lipid droplets and abundant mitochondria that highly express uncoupling protein 1 (UCP1), which is responsible for thermogenesis. Beige adipose tissue (BeAT) is interspersed within WAT depots (especially inguinal subcutaneous fat), which shares numerous similarities with classical BAT, and has piqued the interest of researchers.

Currently, two pharmaceutical approaches are used for regulating obesity: reducing caloric intake (or absorption) or increasing caloric expenditure (thermogenesis). Therefore, research is underway to explore various strategies to increase the quantity and activity of BAT/BeAT, with potential therapeutic applications in the treatment of

obesity and type 2 diabetes. Multiple lines of evidence support a positive association between regular consumption of natural products and fat browning.[4] *Nelumbo nucifera* (lotus) leaf is a medicinal and food species with a wide range of nutritional and phytochemical properties. It contains multiple bioactive components including phenolic acids, flavonoids, alkaloids, terpenoids, steroids and saponins, which is included in weight loss supplements. The underlying anti-obesity mechanisms of lotus leaf have been reported as follows: 1) inhibition of pancreatic lipase activity; 2) inhibition of lipogenesis and inflammation; 3) increase in hepatic lipase activity.[5] However, the role of white-to-beige adipose tissue conversion in its beneficial metabolic actions remains unclear.

Mitophagy has been defined as an autophagic process occurring solely for mitochondria and plays an essential role in obesity. Inhibiting mitophagy *via* genetic manipulation or pharmacological intervention allows brown/beige adipocytes to retain their mitochondria and continue to generate heat through oxidative metabolism, leading to increased energy expenditure. An *in vivo* study demonstrated that suppression of autophagy in brown adipocyte-specific Atg7 knockout mice reduced body weight and improved glucose metabolism.[6] Furthermore, genetic deletion of Atg5/12 could enhance UCP1 and mitochondrial protein expression in the iWAT and thus prevent diet-induced obesity and insulin resistance.[7] Our previous research showed lotus leaf extract (LLE) could induce expression of PGC-1α, SIRT1, and UCP1 during brown adipocyte differentiation.[8] Here, we extend our previous studies integrating cellular and animal experiments to explore the effects of LLE on beige adipocyte formation based on

autophagic mechanisms. Our findings confirm the ability of LLE to induce thermogenic processes in WAT, and support a mechanism through the AMPK/DRP1/mitophagy signaling pathway.

2. Materials and Methods

2.1. Materials

Mouse embryo fibroblast (3T3-L1) cells were purchased from the Cell Bank of the Chinese Academy of Sciences (Kunming, China). Foetal bovine serum (FBS) was purchased from Lonsera (Uruguay). 1-Methyl-3-isobutylxanthine (IBMX) was purchased from Sigma-Aldrich (USA). Dexamethasone (Dex) and insulin (Ins) were purchased from Macklin (Shanghai, China). Janus green B was purchased from Yuanye Bio-Technology Co., Ltd (Shanghai, China). Primary antibodies except β_3-AR (1:1000, ABclonal) and p-DRP1$_{Ser637}$ (1:1000, Affinity) were purchased from Proteintech Group Inc. (Wuhan, China).

2.2. Preparation of LLE

The extraction of the *Nelumbo nucifera* (lotus) leaves (Bozhou, Anhui, China) was performed according to a previous report.[8] Briefly, lotus leaves were extracted in 80% ethanol and subsequently filtered with 0.45 μM membrane, then concentrated and lyophilized to obtain lotus leaf extract (LLE), which was stored at -20°C. The contents of total polyphenols and total flavonoids in LLE were determined as 383.7 μg/mg and 178.3 μg/mg, respectively, in which miquelianin (128.21 μg/mg) was identified as the major phenolic compound.

2.3. Cell culture, differentiation, and treatment

3T3-L1 cells were cultured and differentiated according to our previous method.[9] Briefly, the cells were cultured for 2 days in high-glucose (4.5 g/L D-glucose) medium supplemented with 0.5 mM IBMX, 1 mM DEX, and 10 μg/mL Ins for 2 days, and then replaced with medium containing 10 μg/mL insulin for 6 days until visible lipid droplets appeared. At day 5, different concentration of LLE (50, 100, and 200μg/mL) or rosiglitazone (Rosi, 1μM) were added to the differentiation medium for 4 days.

2.4. Cell viability assay

The viability of 3T3-L1 cells was detected by CCK-8 kit (Beyotime, China). Briefly, different concentrations of LLE were added to cells in 96-well plates and incubated at 37℃ for 24 h. Then, 10 μl of CCK-8 solution was added to each well and incubated at 37℃ for 1 h. The absorbance at 450 nm was measured by a microplate reader.

2.5. Oil Red O and Bodipy 505/515 lipid staining

Oil Red O staining of 3T3-L1 cells was performed consistently with our previous methods.[9] For Bodipy (green) staining, the 3T3-L1 cells were incubated with 0.2 μM Bodipy 505/515 for 15 min. The nuclei were then stained with 1μg/mL DAPI for 1 min. Cells were examined using a fluorescence microscope and photographed.

2.6. Mitochondrial staining

Janus Green B is an indirect method to assess mitochondrial dysfunction as the contents escape in the cytosol upon the rupture of the mitochondrial membrane, leading to colourant oxidation.[10] Briefly, the cells were stained with Janus Green B for 5 minutes, after which they were observed under optical microscopy (Axio Vert.A1, Germany).

2.7. Mitochondrial membrane potential (MMP) staining

3T3-L1 cells were incubated with JC-1 staining (Beyotime) at 37 °C for 0.5 h followed by three washes with JC-1 buffer, followed by observation under a fluorescent microscope (Axio Vert.A1, Germany). MMP value was expressed by the fluorescence ratio of polymer (red) to monomer (green).

2.8. Dichlorofluorescein assay

DCFH-DA was employed to measure intracellular reactive oxygen species (ROS) production in 3T3-L1 cells. 6-well plates were incubated with 1 ml of DCFH-DA (10 μM) at 37 °C for 20 min, and then visualized under a fluorescence microscope (Axio Vert.A1, Germany).

2.9. Determination of NADH content, NAD^+ content, and NAD^+/NADH ratio

The NAD^+/NADH Quantification Kit (Beyotime) was used for the determination of NADH content, NAD^+ content, and NAD^+/NADH ratio according to our previous report.[11]

2.10. Mitophagy assay

The 3T3-L1 cells were co-cultured with LLE and carbonyl cyanide-4-(trifluoromethoxy)phenylhydrazone (FCCP, 10 μM) (an inducer of PINK1/PARKIN mitophagy)[12] at 37°C for 1 h. After removing the medium, 1 mL of monodansylcadaverine (MDC) staining solution was added for incubation at 37°C for 30 min. Photographs were taken following three washes with assay buffer.

2.11. Animals and experimental diets

Male C57BL/6J mice (5-weeks-old) were supplied by Witonglihua Laboratory Animal

Technology Co., Ltd. (Beijing, China) and housed with the approval of the Animals Center of Jiangnan University (JN.No20220615c1100925[233]). All mice were free to feed and drink water. After acclimatization for one week, 40 mice were randomized into ND group fed with normal diet; HFD group (n=8) fed with high-fat diet; LLE-L, LLE-H, and MI groups fed with HFD and orally administered with 100 mg/kg LLE, 200 mg/kg LLE, or 5 mg/kg miglitol, respectively, for 12 weeks. Detailed ingredients in ND and HFD are described in Supplemental Table 1. Body weight was recorded weekly and food intake was recorded every 3 days.

2.12. Blood biochemical and body temperature analysis

Fasting blood glucose (FBG) levels were measured in blood obtained from the tail vein of mice fasted for 12 hours. Serum was obtained by centrifuging blood at 3500 g for 10 minutes obtained from mouse eyeballs under anesthesia, and then stored at -80 °C before being subjected to biochemical analysis as previously reported.[9] In addition, mice were maintained in a 4°C environment and rectal temperatures were measured with a digital thermometer (Hainuo, Qingdao, China) after 1-4 hours.

2.13. Histology and immunolabeling analysis

Paraffin sections (5 μm) of the eWAT (epididymal WAT), iWAT (inguinal WAT), liver, spleen, and kidney were stained with haematoxylin and eosin (H&E) for histopathological analysis. Immunohistochemistry/immunofluorescence was carried out following the PV9000 Immunohistochemistry Kit (Servicebio). The procedure involved 1) permeabilization; 2) serum blocking; 3) primary antibody incubation; 4) secondary antibody incubation; 5) DAPI counter-staining of cell nuclei; 6) mounting;

and 7) image capture.[13]

2.14. Real-time quantitative PCR (qPCR) and Western blotting analysis

The total RNA extraction, cDNA synthesis, and qPCR were performed as previously described.[8] The primer sequences are listed in Supplemental Table 2. Western blotting was conducted as described in our previous study (2-3 randomly selected samples from each group were mixed into one sample for protein extraction).[8] The target proteins were blotted on a PVDF membrane and probed with rabbit primary antibodies, followed by incubation with secondary antibodies. The quantitative analysis was performed using Image J software (NIH, Bethesda, MD, USA).

2.15. Statistical analysis

Data from individual experiments are presented as means ± standard deviation. Statistical significance was calculated using one-way analysis of variance with Duncan's test. Values of $p<0.05$ were considered to be statistically significant.

3. Results

3.1. Effects of LLE on the viability of 3T3-L1 cells

The viability of 3T3-L1 cells was measured following treatment with LLE for 24 hours. Cells treated with LLE (50-800 μg/mL) showed similar viability to untreated cells (Fig. 1A), indicating that LLE was not significantly toxic to 3T3-L1 cells in this concentration range.

3.2. LLE promotes lipolysis in 3T3-L1 cells

Oil Red O and Bodipy 505/515 staining revealed that lipid droplet accumulation was

dose-dependently reduced in LLE-stimulated cells (Fig. 1B and 1C). By Western blotting analysis, we found that LLE significantly potentiated the protein expression levels of adipose triglyceride lipase (ATGL), abhydrolase domain 5-containing (ABHD5), and Perilipin 5 (PLIN5), approaching the positive control Rosi (1 μM) (Fig. 1D and 1E), suggesting the lipolytic potential of LLE.

3.3. LLE potentiates mitochondrial activity in 3T3-L1 cells

Janus green B staining determines mitochondrial membrane stability, and the deeper blue/green coloration in LLE-treated cells demonstrates that LLE enhanced mitochondrial activity (Fig. 2A). ROS is both a product and target of mitochondria, and our results demonstrated a decreased level of ROS in LLE-treated 3T3-L1 cells (Fig. 2B and 2D). Furthermore, LLE treatment could increase MMP level, as indicated by the high aggregates (red)/monomers (green) ratio, which was equivalent to the Rosi group (Fig. 2C and 2E-G). Nicotinamide adenine dinucleotide (NAD^+) serves as an important coenzyme in cellular energy metabolism and redox reactions in mitochondrial function.[14] Here, NADH levels exhibited no change, but NAD^+ significantly increased compared with that in the control (Con) (Fig. 2H and 2I). Thus, high NAD+/NADH ratios (Fig. 2J) accompanied by high protein expression of nicotinamide-phosphate ribosyltransferase (NAMPT), an enzyme essential for NAD^+ biosynthesis (Fig. 2K), were observed in LLE-stimulated cells.

3.4. LLE promotes mitochondrial biogenesis and adipocyte beiging in 3T3-L1 cells

Indicators associated with mitochondrial biogenesis were assessed by qPCR and Western blotting. The results showed mRNA levels of *Nrf1*, *Tfam*, *PPARα*, cytochrome

oxidase subunit VII a (*Cox7a*), *Cox2*, and *Cox-IV* were dose-dependently increased by LLE treatment (Fig. 3A). The high protein expression of TFAM and COX-IV was correspondingly observed in LLE-treated cells (Fig. 3B and 3C). These data demonstrated that LLE contributed to mitochondrial biogenesis, and this may be attributed to its induction of the beiging process. This is supported by the significant up-regulation of beige fat-enriched genes (e.g., *Sirt1*, *Pgc-1α*, *Cidea*, *Ucp1*, *Cd40*, *Cd147*, *Cited1*, and *Fgf21*) observed in the LLE-treated cells (Fig. 3A). The higher expression of SIRT1, PGC-1α, and UCP1 in LLE-treated cells was also demonstrated by Western blotting (Fig. 3B and 3C). Meanwhile, immunofluorescence detection of SIRT1 (Fig. 3D) and UCP1 (Fig. 3E) also showed a similar trend. Furthermore, we found LLE significantly increased the expression of β_3-AR and the ratios of p-AMPKα/AMPKα and p-ACC/ACC (Fig. 3F and 3G). However, we found p-p38/p38 ratio exhibited a declining trend in LLE-treated cells (Fig. 3F and 3G); therefore, we propose that the positive action of LLE is via β_3-AR/AMPK signaling.

3.5. LLE inhibites PINK1/PARKIN-mediated mitophagy in 3T3-L1 cells

As shown in Fig. 4A, LLE could inhibit MDC staining indicating a reduction in mitophagy. Further data support the role of PINK1/PARKIN-mediated mitophagy with decreased mRNA expression of autophagy-related genes (e.g., *Pink1*, *Parkin*, *Beclin1*, and *LC3B*) and up-regulation of p62 expression in LLE-stimulated cells (Fig. 4B). The same phenomenon was also demonstrated by Western blotting (Fig. 4C-G). Notably, an increase expression of the pro-fission protein p-DRP1 was also identified in LLE-treated cells (Fig. 4H).

3.6. LLE improves obesity- and lipid-related indicators in HFD-fed mice

LLE treatment ameliorated HFD-induced increase in weight gain (Fig. 5A), liver weight (Fig. 5C), eWAT/body weight (Fig. 5F), perirenal WAT (pWAT)/body weight (Fig. 5G), and iWAT/body weight (Fig. 5H) and was comparable to that of the MI group. Moreover, food intake (Fig. 5B), spleen weight (Fig. 5C) and kidney weight (Fig. 5D), as well as BAT/body weight (Fig. 5I) exhibited no significant differences among the groups. Blood biochemical analysis revealed that LLE supplementation improved HFD-induced glycolipid disorders such as decreased FBG, triglycerides (TG), total cholesterol (TC), and low-density lipoprotein cholesterol (LDL-C) levels and increased high-density lipoprotein cholesterol (HDL-C) levels (Fig. 5J-N), with very similar effects to MI treatment. Meanwhile, we also found LLE-treated mice exhibited a higher rectal temperature upon cold exposure (Fig. 5O), indicating the ability of LLE to enhance body adaptation by generating more heat.

3.7. Tissue histopathological analysis of LLE-treated mice

As shown in Fig. 6A-D, LLE treatment reduced the size of adipocytes within eWAT, iWAT, and BAT, reaching a level similar to that of the MI group. Hepatic H&E staining (Fig. 6A) together with the results of NAFLD activity scores (NAS devised by NASH CRN)[15] (Fig. 6E) showed that LLE treatment reduced HFD-induced lipid deposition. Histological sections of kidney and spleen of mice were used to further investigate the safety of LLE, and the results showed no significant difference in kidney and spleen among groups, indicating that neither low nor high doses of LLE caused damage to kidney and spleen of mice (Fig. 6A).

3.8. LLE indues beiging and mitochondrial biogenesis in iWAT of HFD-fed mice

qPCR analysis of beige and mitochondrial biogenesis-related genes of iWAT revealed that different doses of LLE upregulated the mRNA levels of *Sirt1, Pgc-1α, Prdm16, Dio2, Ucp1, Nrf1, Tfam, Cox2, Tmem26, Cd137, Cd40, and Tbx1* (Fig. 7A). Immunohistochemistry demonstrated higher levels of SIRT1 and UCP1 in LLE-treated iWAT, which was consistent with the mRNA expression assay (Fig. 7B). Meanwhile, Western blotting showed LLE markedly increased β_3-AR, SIRT1, TFAM, and UCP1 protein expression, as well as p-AMPKα/AMPKα ratio (Fig. 7C and 7D). Collectively, these results evidence that LLE promotes beiging of white adipocytes and induces mitochondrial biogenesis.

3.9. Role of AMPK/DRP1/mitophagy in LLE-induced adipocyte beiging

Western blotting (Figure 8A and 8B) analysis showed that LLE could increase the ratio of p-DRP1/DRP1, downregulate the expression of autophagy proteins (e.g., PINK1, PARKIN, BECLIN1, and LC3B) and upregulate the expression of p62 compared to the HFD group, which suggests that LLE has an inhibitory effect on mitophagy. For AMPK signaling investigation, cells were pre-incubated with AMPK inhibitor Compound C (5 μM) or activator AICAR (10 μM) for 24 h. Immunofluorescence revealed that the increased UCP1 by LLE could be further enhanced by pretreatment with AICAR, but Com C reversed this trend (Fig. 8C). Furthermore, Western blotting results demonstrated that Comp C could inhibit LLE-induced downregulation of autophagy-related proteins (PINK1, PARKIN, BECLIN1, and LC-3B) and upregulation of p-DRP1 and beige fat-related markers such as SIRT1, PGC-1α, COX-2, and UCP1. In

287 contrast to Compound C, AICAR largely enhanced the changes in the above indicators
288 instigated by LLE treatment (Fig. 8D and 8E).
289
290 **4. Discussion**
291 Beige fat mainly occurs in inguinal WAT depots and the search for natural products to
292 induce beiging of white fat may contribute to intervention and treatment of obesity.
293 Lotus leaf, which includes multiple functional components such as flavonoids and
294 alkaloids, exhibits promising anti-obesity effects, and the browning of fat may be an
295 important pathway for its effects. The process of lipolysis is a prerequisite step for
296 thermogenesis in brown and beige adipocytes.[16] CGI58/ABHD5 is a lipid droplet-
297 associated ATGL activator that interacts with PLINs to regulate basal and stimulated
298 lipolysis. Subsequently, free fatty acids released by lipolysis can activate UCP1 to drive
299 mitochondrial thermogenesis.[17] Here, LLE reduced lipid droplet accumulation by
300 increasing lipolysis in 3T3-L1 cells, which may be responsible for WAT beiging.
301 Mitochondria are key metabolic organelles, and the increase in their activity (e.g.,
302 mitochondrial biogenesis) is positively associated with the conversion of white-to-
303 beige adipocytes.[19] The high MMP implies elevated mitochondrial activity, whereas
304 ROS accumulation impairs or inhibits UCP1 activity.[18] Measurement of MMP and ROS
305 production indicates that LLE enhanced mitochondrial function. Moreover,
306 mitochondrial metabolism is strongly dependent on the redox coupling of
307 NAD^+/NADH.[19] In our study, the levels of NAD^+ and its biosynthetic enzyme NAMPT
308 were markedly elevated in LLE-stimulated cells, which is consistent with an earlier

observation of increase in NAD^+ levels during beige adipogenesis.[20] Activation of β_3-AR/AMPK signaling has recently been revealed to enhance SIRT1 activity by increasing cellular NAD^+ levels, inducing deacetylation of PGC-1α and mitochondrial biogenesis.[21,22] Moreover, PRDM16 as a transcriptional co-activator of PGC-1α can enhance expression of genes important for mitochondrial biogenesis and uncoupling.[23-25] Here, the increase in β_3-AR expression and AMPK phosphorylation with LLE treatment was followed by upregulated UCP1, PRDM16, SIRT1 and PGC-1α supporting that LLE could induce white fat beiging and mitochondrial biogenesis *via* regulation of β_3-AR/AMPK signaling. This is consistent with our previous findings that LLE induces brown-like adipocytes in $C_3H_{10}T_{1/2}$ cells through activation of β_3-AR/AMPK signaling.[8]

Recent studies have found that autophagy is increased in patients with obesity and diabetes, and that inhibiting autophagy in adipocytes by targeted deletion of autophagic genes in mice improves the obesity phenotype. Furthermore, upon blockade of mitophagy in white adipocytes, mitochondria failed to degrade and simultaneously inhibited lipogenesis, resulting in a beige/brown adipocyte features.[26] Evidence suggests that liensinine or raspberry ketone effectively impede beige-to-white adipocyte transition by blocking mitophagy, ultimately leading to the maintenance of beige-like features (e.g., UCP1, PRDM16, PGC-1α) in 3T3-L1 cells.[27-28] Research has recently revealed that PINK1 and PARKIN jointly function in the mitochondrial quality control pathway, whereby damaged mitochondria are removed *via* an autophagic process known as 'mitophagy'.[29] It was found that mangiferin retains thermogenic

capacity by down-regulating PINK1-PARKIN mediated mitophagy during brown adipocyte differentiation.[29] UCP1 expression was highly induced in the gonadal WAT of PARKIN-deficient mice after treatment with CL 316,243, a β3-adrenergic receptor agonist. Moreover, differentiated 3T3-L1 adipocytes transfected with mCherry-PARKIN displayed an impaired browning response.[30] Consistent with these studies, sesamol was shown to potentiate 3T3-L1 browning and mitochondrial biogenesis by inhibiting PINK1/PARKIN mitophagy.[31] Available evidence supports that miquelianin could increase mitochondrial mass and attenuate autophagy in high glucose-induced hypertrophic 3T3-L1 adipocytes.[32] Our previous findings also demonstrated that PINK1/PARKIN mitophagy could be inhibited by miquelianin in high-glucose cultured 3T3-L1 adipocytes, which in turn allowed for the browning process.[33] Here, significant suppression of mitophagy was demonstrated in miquelianin-rich LLE-treated 3T3-L1 cells and iWAT, suggesting PINK1-PARKIN signaling as a key pathway underlying LLE-induced beiging.

Inactivation of DRP1, a major regulator of mitochondrial dynamics, reverses high-glucose-induced MMP downregulation and diminishes mitochondrial fission.[34] In vitro and in vivo data indicate that increased DRP1 activity in adipose tissue is identified as an essential contributor to mitochondrial dysfunction during obesity.[35] It was identified that the PGC-1α and UCP1 expression, mtDNA content, and AMPKα phosphorylation were significantly upregulated in WAT of Leptin or Mdvi-1 (a selective inhibitor of DRP1 fission-protein)-treated ob/ob mice as compared with the untreated group. Moreover, in WAT isolated adipocytes, DRP1 blockade by siRNA DRP1 also increased

oxidative metabolism and mitochondrial function, indicating the potential role of DRP1 in "browning" of WAT.[36] Importantly, DRP1 was found to function as an enhancer of PARKIN and PINK1,[37] and its inactivation diminished PINK, PARKIN, and LC3II expression.[38] Suppression of mitophagy by DRP1 silencing/knockdown has also been observed in other cells.[39-43] DRP1 function can be subject to regulation by AMPK activation through the reduction of DRP1 expression or phosphorylation of DRP1 at serine 637.[44, 45] Under high glucose (33 mM) conditions, metformin or resveratrol was found to activate AMPK and increase basal DRP1 phosphorylation (Ser 637) in 3T3-L1 cells differentiated for 8-10 days, but knockdown of AMPKα blocked DRP1 phosphorylation and mitochondrial fission.[46] The AMPK/DRP1 pathway was identified as a regulator of mitochondrial function, as shown by the findings of Zhou et al. that AICAR prevents the overproduction of mitochondrial ROS and reduces MMP production by inhibiting DRP1 activity.[47] Our prior study revealed that miquelianin facilitated beige fat formation by phosphorylating AMPK and DRP1 at serine 637,[32] which in combination with the findings from the present study suggests that miquelianin-rich LLE may induce WAT beiging through the AMPK/DRP1-PINK1/PARKIN signaling axis.

5. Conclusions

LLE endowed the white adipocytes with similar features to those of brown adipocytes. The induction of beige adipocyte formation and mitochondrial biogenesis were dependent on AMPK/DRP1/PINK1/PARKIN signaling. Our results demonstrate the

potential of lotus leaves in enhancing energy expenditure *via* recruiting beige adipocytes in white fat.

Declarations of competing interest

The authors declare no conflicts of interest.

Acknowledgments

The authors acknowledge financial support from the National Key Research and Development Program of China (No. 2022YFF1100204), the National Natural Science Foundation of China (No. 31771978), and the Six Talent Peaks Project in Jiangsu Province (No. NY-095).

References

1. Tseng YH, Cypess AM and Kahn CR, Cellular bioenergetics as a target for obesity therapy. *Nat Rev Drug Discov* **9**:465-482 (2010).
2. Zhang Z, Zhang H, Li B, Meng X, Wang J, Zhang Y, Yao S, Ma Q, Jin L, Yang J, Wang W and Ning G, Berberine activates thermogenesis in white and brown adipose tissue. *Nat Commun* **5**:5493 (2014).
3. Wang Z, Zeng M, Wang Z, Qin F, Wang Y, Chen J, Christian M and He Z, Food phenolics stimulate adipocyte browning via regulating gut microecology. *Crit Rev Food Sci*:1-27 (2021).
4. Hu J, Wang Z, Tan BK and Christian M, Dietary polyphenols turn fat "brown": A narrative review of the possible mechanisms. *Trends Food Sci Tech* **97**:221-232 (2020).
5. Wang Z, Cheng Y, Zeng M, Wang Z, Qin F, Wang Y, Chen J and He Z, Lotus (Nelumbo nucifera Gaertn.) leaf: A narrative review of its Phytoconstituents, health benefits and food industry applications. *Trends Food Sci Tech* **112**:631-650 (2021).
6. Kim D, Kim JH, Kang YH, Kim JS, Yun SC, Kang SW and Song Y, Suppression of Brown Adipocyte Autophagy Improves Energy Metabolism by Regulating Mitochondrial Turnover. *Int J Mol Sci* **20**:3520 (2019).
7. Altshuler-Keylin S, Shinoda K, Hasegawa Y, Ikeda K, Hong H, Kang Q, Yang Y, Perera RM, Debnath J and Kajimura S, Beige Adipocyte Maintenance Is Regulated by Autophagy-Induced Mitochondrial Clearance. *Cell Metab* **24**:402-419 (2016).
8. Wang Z, Xue C, Wang X, Zeng M, Wang Z, Chen Q, Chen J, Christian M and He ZJFRI, Quercetin 3-O-glucuronide-rich lotus leaf extract promotes a Brown-fat-phenotype in C3H10T1/2 mesenchymal stem cells. *Food Res Int* **163**:112198 (2023).
9. Wang Z, Hu J, Hamzah SS, Ge S, Lin Y, Zheng B, Zeng S, Lin S, n-Butanol extract of lotus seeds exerts antiobesity effects in 3T3-L1 preadipocytes and high-fat diet-fed mice via activating adenosine monophosphate-activated protein kinase. *J. Agric Food Chem* **67**:1092-1103 (2019).
10. Daw S and Law S, Quercetin induces autophagy in myelodysplastic bone marrow including hematopoietic stem/progenitor compartment. *Environ Toxicol* **36**:149-167 (2021).
11. Wang Z, Chaoyi X, Yang T, Wang Z, Chen Q, Chen J and he Z, Miquelianin, a main functional flavonoid of lotus leaf, induces thermogenic signature via p38-PINK1-PARKIN-mediated mitophagy and mimicking NRF2 signaling during brown adipocyte differentiation. *Food Frontiers* **0**: 1-14. (2023).
12. Strappazzon F, Nazio F, Corrado M, Cianfanelli V, Romagnoli A, Fimia GM, Campello S, Nardacci R, Piacentini M, Campanella M and Cecconi F, AMBRA1 is able to induce mitophagy via LC3 binding, regardless of PARKIN and p62/SQSTM1. *Cell Death Differ* **22**:419-432 (2015).
13. Liu, C., Gao, W., Zhao, L., Cao, Y.J.A., 2022. Progesterone attenuates neurological deficits and exerts a protective effect on damaged axons via the PI3K/AKT/mTOR-dependent pathway in a mouse model of intracerebral hemorrhage. *Aging* 14(6), 2574.
14. Yamaguchi S, Franczyk MP, Chondronikola M, Qi N, Gunawardana SC, Stromsdorfer KL, Porter LC, Wozniak DF, Sasaki Y, Rensing N, Wong M, Piston DW, Klein S and Yoshino J, Adipose tissue NAD^+ biosynthesis is required for regulating

adaptive thermogenesis and whole-body energy homeostasis in mice. *Proc Natl Acad Sci USA* **116**:23822-23828 (2019).
15. Kleiner DE, Brunt EM, Van Natta M, Behling C, Contos MJ, Cummings OW, Ferrell LD, Liu YC, Torbenson MS and Unalp-Arida AJH, Design and validation of a histological scoring system for nonalcoholic fatty liver disease. *Hepatology* **41**:1313-1321 (2005).
16. Lim S, Park J and Um JY, Ginsenoside Rb1 Induces Beta 3 Adrenergic Receptor-Dependent Lipolysis and Thermogenesis in 3T3-L1 Adipocytes and db/db Mice. *Front Pharmacol* **10**:1154 (2019).
17. Barneda D, Frontini A, Cinti S and Christian M, Dynamic changes in lipid droplet-associated proteins in the "browning" of white adipose tissues. *BBA-Mol Cell Biol L* **1831**:924-933 (2013).
18. Pisani DF, Barquissau V, Chambard JC, Beuzelin D, Ghandour RA, Giroud M, Mairal A, Pagnotta S, Cinti S, Langin D and Amri EZ, Mitochondrial fission is associated with UCP1 activity in human brite/beige adipocytes. *Mol Metab* **7**:35-44 (2018).
19. Kory N, Uit de Bos J, van der Rijt S, Jankovic N, Güra M, Arp N, Pena IA, Prakash G, Chan SH, Kunchok T, Lewis CA and Sabatini DM, MCART1/SLC25A51 is required for mitochondrial NAD transport. *Sci. Adv.* **6** (2020).
20. Jia R, Wei X, Jiang J, Yang Z, Huang J, Liu J, Yan J and Luo X, NNMT is induced dynamically during beige adipogenesis in adipose tissues depot-specific manner. *J Physiol Biochem* **78**:169-183 (2022).
21. Jang MH, Kang NH, Mukherjee S, Yun JWJB and Engineering B, Theobromine, a methylxanthine in cocoa bean, stimulates thermogenesis by inducing white fat browning and activating brown adipocytes. *Biotechnol Bioprocess Eng* **23**:617-626 (2018).
22. Kang NH, Mukherjee S, Min T, Kang SC and Yun JWJB, Trans-anethole ameliorates obesity via induction of browning in white adipocytes and activation of brown adipocytes. *Biochimie* **151**:1-13 (2018).
23. Seale P, Kajimura S, Yang W, Chin S, Rohas LM, Uldry M, Tavernier G, Langin D and Spiegelman BM, Transcriptional control of brown fat determination by PRDM16. *Cell Metab* **6**:38-54 (2007).
24. de Mello AH, Costa AB, Engel JDG and Rezin GT, Mitochondrial dysfunction in obesity. *Life Sci.* **192**:26-32 (2018).
25. Cho SY, Lim S, Ahn KS, Kwak HJ, Park J and Um J-Y, Farnesol induces mitochondrial/peroxisomal biogenesis and thermogenesis by enhancing the AMPK signaling pathway in vivo and in vitro. *Pharmacol. Res.* **163**:105312 (2021).
26. Ro SH, Jang Y, Bae J, Kim IM, Schaecher C and Shomo ZD, Autophagy in Adipocyte Browning: Emerging Drug Target for Intervention in Obesity. *Front Physiol* **10**:22 (2019).
27. Xie S, Li Y, Teng W, Du M, Li Y and Sun B, Liensinine Inhibits Beige Adipocytes Recovering to white Adipocytes through Blocking Mitophagy Flux In Vitro and In Vivo. *Nutrients* **11**:1640 (2019).
28. Leu S-Y, Tsai Y-C, Chen W-C, Hsu C-H, Lee Y-M and Cheng P-Y, Raspberry

485 ketone induces brown-like adipocyte formation through suppression of autophagy in
486 adipocytes and adipose tissue. *J. Nutr. Biochem.* **56**:116-125 (2018).
487 29. Rahman MS and Kim Y-S, PINK1–PRKN mitophagy suppression by mangiferin
488 promotes a brown-fat-phenotype via PKA-p38 MAPK signalling in murine C3H10T1/2
489 mesenchymal stem cells. *Metabolism* **107**:154228 (2020).
490 30. Taylor D and Gottlieb RA, Parkin-mediated mitophagy is downregulated in
491 browning of white adipose tissue. *Obesity* **25**:704-712 (2017).
492 31. Lin C, Chen J, Hu M, Zheng W, Song Z and Qin H, Sesamol promotes browning
493 of white adipocytes to ameliorate obesity by inducing mitochondrial biogenesis and
494 inhibition mitophagy via β3-AR/PKA signaling pathway. *Food Nutr Res* **65** (2021).
495 32. Herranz-López M, Olivares-Vicente M, Rodríguez Gallego E, Encinar JA, Pérez-
496 Sánchez A, Ruiz-Torres V, Joven J, Roche E and Micol V, Quercetin metabolites from
497 Hibiscus sabdariffa contribute to alleviate glucolipotoxicity-induced metabolic stress in
498 vitro. *Food Chem Toxicol* **144**:111606 (2020).
499 33. Wang Z, Yang T, Zeng M, Wang Z, Chen Q, Chen J, Christian M and He Z,
500 Miquelianin in Folium Nelumbinis extract promotes white-to-beige fat conversion via
501 blocking AMPK/DRP1/mitophagy and modulating gut microbiota in HFD-fed mice.
502 *Food Chem Toxicol* 181:114089 (2023).
503 34. Zhang MY, Zhu L, Bao X, Xie TH, Cai J, Zou J, Wang W, Gu S, Li Y, Li HY, Yao
504 Y and Wei TT, Inhibition of Drp1 ameliorates diabetic retinopathy by regulating
505 mitochondrial homeostasis. *Exp Eye Res* **220**:109095 (2022).
506 35. Xia W, Veeragandham P, Cao Y, Xu Y, Rhyne T, Qian J, Hung CW, Zhao P, Jones
507 Y, Gao H, Liddle C, Yu R, Downes M, Evans R, Ryden M, Wabitsch M, Reilly S, Huang
508 J and Saltiel A, Obesity-dependent increase in RalA activity disrupts mitochondrial
509 dynamics in white adipocytes. *Research square* (2023).
510 36. Finocchietto P, Perez H, Blanco G, Miksztowicz V, Marotte C, Morales C, Peralta
511 J, Berg G, Poderoso C, Poderoso J, and Carreras, M, aInhibition of mitochondrial
512 fission by Drp-1 blockade by short-term leptin and Mdivi-1 treatment improves white
513 adipose tissue abnormalities in obesity and diabetes. *Pharmacol Res* **178**:106028
514 (2022).
515 37. Poole AC, Thomas RE, Andrews LA, McBride HM, Whitworth AJ and Pallanck
516 LJ, The PINK1/Parkin pathway regulates mitochondrial morphology. *Proc Natl Acad*
517 *Sci U S A* **105**:1638-1643 (2008).
518 38. Tanaka A, Cleland MM, Xu S, Narendra DP, Suen DF, Karbowski M and Youle RJ,
519 Proteasome and p97 mediate mitophagy and degradation of mitofusins induced by
520 Parkin. *J Cell Biol* **191**:1367-1380 (2010).
521 39. Wu H, Li G, Chen W, Luo W, Yang Z, You Z and Zou Y, Drp1 knockdown represses
522 apoptosis of rat retinal endothelial cells by inhibiting mitophagy. *Acta Histochem*
523 **124**:151837 (2022).
524 40. Lee Y, Lee H-Y, Hanna RA and Gustafsson ÅB, Mitochondrial autophagy by Bnip3
525 involves Drp1-mediated mitochondrial fission and recruitment of Parkin in cardiac
526 myocytes. *Am J Physiol Heart Circ Physiol* 301:H1924-H1931 (2011)
527 41. Pernaute B, Pérez-Montero S, Sánchez Nieto JM, Di Gregorio A, Lima A, Lawlor
528 K, Bowling S, Liccardi G, Tomás A, Meier P, Sesaki H, Rutter GA, Barbaric I and

Rodríguez TA, DRP1 levels determine the apoptotic threshold during embryonic differentiation through a mitophagy-dependent mechanism. *Dev. Cell* **57**:1316-1330.e1317 (2022).
42. Park YS, Choi SE and Koh HC, PGAM5 regulates PINK1/Parkin-mediated mitophagy via DRP1 in CCCP-induced mitochondrial dysfunction. *Toxicol Lett* **284**:120-128 (2018).
43. Buhlman L, Damiano M, Bertolin G, Ferrando-Miguel R, Lombès A, Brice A and Corti O, Functional interplay between Parkin and Drp1 in mitochondrial fission and clearance. *Biochimica et Biophysica Acta (BBA) - Molecular Cell Research* **1843**:2012-2026 (2014).
44. Tong W, Leng L, Wang Y, Guo J, Owusu FB, Zhang Y, Wang F, Li R, Li Y, Chang Y, Wang Y and Wang Q, Buyang huanwu decoction inhibits diabetes-accelerated atherosclerosis via reduction of AMPK-Drp1-mitochondrial fission axis. Journal of Ethnopharmacology 312:116432 (2023).
45. Li J, Wang Y, Wang Y, Wen X, Ma XN, Chen W, Huang F, Kou J, Qi LW, Liu B and Liu K, Pharmacological activation of AMPK prevents Drp1-mediated mitochondrial fission and alleviates endoplasmic reticulum stress-associated endothelial dysfunction. *J Mol Cell Cardiol* **86**:62-74 (2015).
46. Li A, Zhang S, Li J, Liu K, Huang F and Liu B, Metformin and resveratrol inhibit Drp1-mediated mitochondrial fission and prevent ER stress-associated NLRP3 inflammasome activation in the adipose tissue of diabetic mice. *Mol Cell Endocrinol* **434**:36-47 (2016).
47. Zhou Y, Li M, Wang Z, Lin X, Xu Y, Feng S and Miao J, AMPK/Drp1 pathway mediates Streptococcus uberis-Induced mitochondrial dysfunction. *Int. Immunopharmacol*. 113:109413 (2022).

Figure Legends

Fig. 1. Effect of LLE on lipolysis in 3T3-L1 cells. (A) the effect of LLE on the viability of 3T3-L1 cells. (B) Oil Red O and Bodipy/DAPI staining (×200) (C) Fluorescence intensity of the Bodipy-stained lipid droplets. (D and E) Western blotting analysis of the expression of lipolysis-related proteins (ATGL, ABHD5, and PLIN5) (n=2).

Fig. 2. Effect of LLE on mitochondrial activity in 3T3-L1 cells. (A) Janus green B staining of mitochondria. (B and D) ROS was assessed by the DCF-DA assay (×200) and quantified analysis. (C and E-G) MMP staining with JC-1 (×200) and quantified analysis.. (H–J) Determination of NADH content, NAD^+ content, and NAD^+/NADH ratio. (K) NAMPT protein expression was measured by Western blotting (n=2).

Fig. 3. Effect of LLE on beige fat formation in 3T3-L1 cells. (A) qPCR analysis of mitochondrial biogenesis-related genes (e.g., *Sirt1*, *Pgc-1α*, *Prdm16*, *Cideα*, *Ucp1*, *Pparα*, *Cox7a, Cox2*, *Nrf1*, *Tfam*, *Cd40*, *Cd147*, *Cited1*, and *Fgf21*) (n=3). (B and C) Western blot analysis of protein expression of SIRT1, PGC-1α, UCP1, COX-IV, and TFAM. (D and E) Immunofluorescence staining of SIRT1 and UCP1 (×400). (F and G) Western blot analysis of Protein expression of β_3-AR, (p)AMPKα, (p)ACC, and (p)p38 in LLE-treated 3T3-L1 cells (n=2).

Fig. 4. Effect of LLE on the PINK/PARKIN mitophagy in 3T3-L1 cells. (A) The fluorescence images of mitophagy caused by FCCP (10 μM) for 24 h. (B) qPCR analysis of mitophagy-related genes (*Pink1*, *Parkin*, *Beclin1*, *LC-3B,* and *p62*) (n=3). (C-H) Western blotting analysis of mitofission protein p-DRP1 and mitophagy-related proteins (PINK1, PARKIN, BECLIN1, LC-3B, and LC-3A) (n=2).

Fig. 5. Effects of LLE on body measurements and serum biochemical indicators. (A)

Body weight was monitored weekly for 12 weeks. (B) Food intake. (C) Liver weight. (D) Spleen weight. (E) Kidney weight. (F) eWAT/body weight. (G) pWAT/body weight. (H) iWAT/body weight. (I) iWAT/body weight. (J) TG. (K) TC. (L) LDL-C. (M) HDL-C. (N) FBG. (O) Rectal temperature.

Fig. 6. Effects of LLE on tissue histology in HFD-fed mice. (A-E) H&E staining of eWAT, iWAT, liver, spleen, and kidney. (F and G) adipocyte size of eWAT and iWAT. (H) NAFLD activity scores.

Fig. 7. LLE stimulates WAT beiging in HFD-fed mice. (A) qPCR analysis of beige and mitochondrial biogenesis-related genes (*Sirt1*, *Pgc-1α*, *Prdm16*, *Dio2*, *Ucp1*, *Nrf1*, *Tfam*, *Cox2*, *Cd137*, *Tmen26*, *Cd40*, and *Tbx1*) (n=3). (B) Immunofluorescence staining of SIRT1 and UCP1. (C and D) Western blotting analysis of the expression of beige fat-related proteins (PGC-1α, COX2, TFAM, and UCP1) (n=2).

Fig. 8. LLE stimulates white adipocyte beiging and mitochondrial biogenesis through AMPK/DRP1-mediated mitophagy. (A and B) Western blotting analysis of the mitophagy-related proteins in iWAT of HFD-fed mice (n=2). (C) Immunofluorescence staining of UCP1 (×400) in LLE-treated 3T3-L1 cells stimulated with or without Com C or AICAR. (D and E) Western blotting analysis of mitophagy and beige fat-related proteins (p-DRP1, PINK1, PARKIN, BECLIN1, LC-3B, SIRT1, PGC-1α, COX-2, and UCP1) in LLE-treated 3T3-L1 cells stimulated with or without Com C or AICAR (n=2).

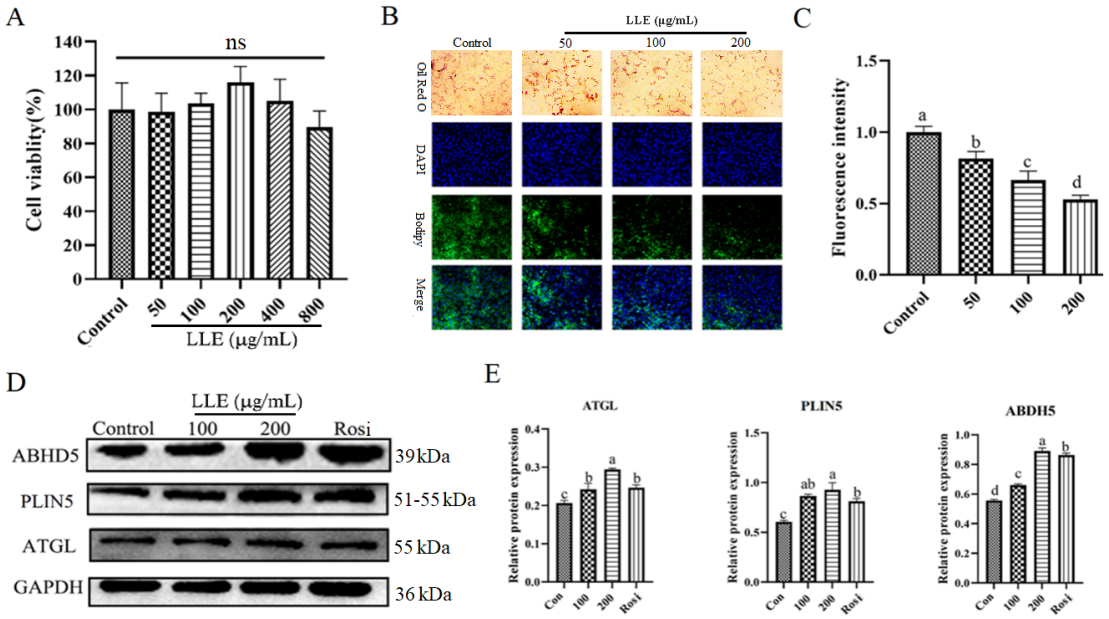
A
ns
Cell viability(%)
Control
50
100
200
400
800
LLE (μg/mL)
B
LLE (μg/mL)
Control
50
100
200
Oil Red O
DAPI
Bodipy
Merge
C
Fluorescence intensity
Control
50
100
200
D
LLE (μg/mL)
Control
100
200
Rosi
ABHD5
PLIN5
ATGL
GAPDH
39 kDa
51-55 kDa
55 kDa
36 kDa
E
ATGL
PLIN5
ABDH5
Relative protein expression
Con
100
200
Rosi

Fig. 1

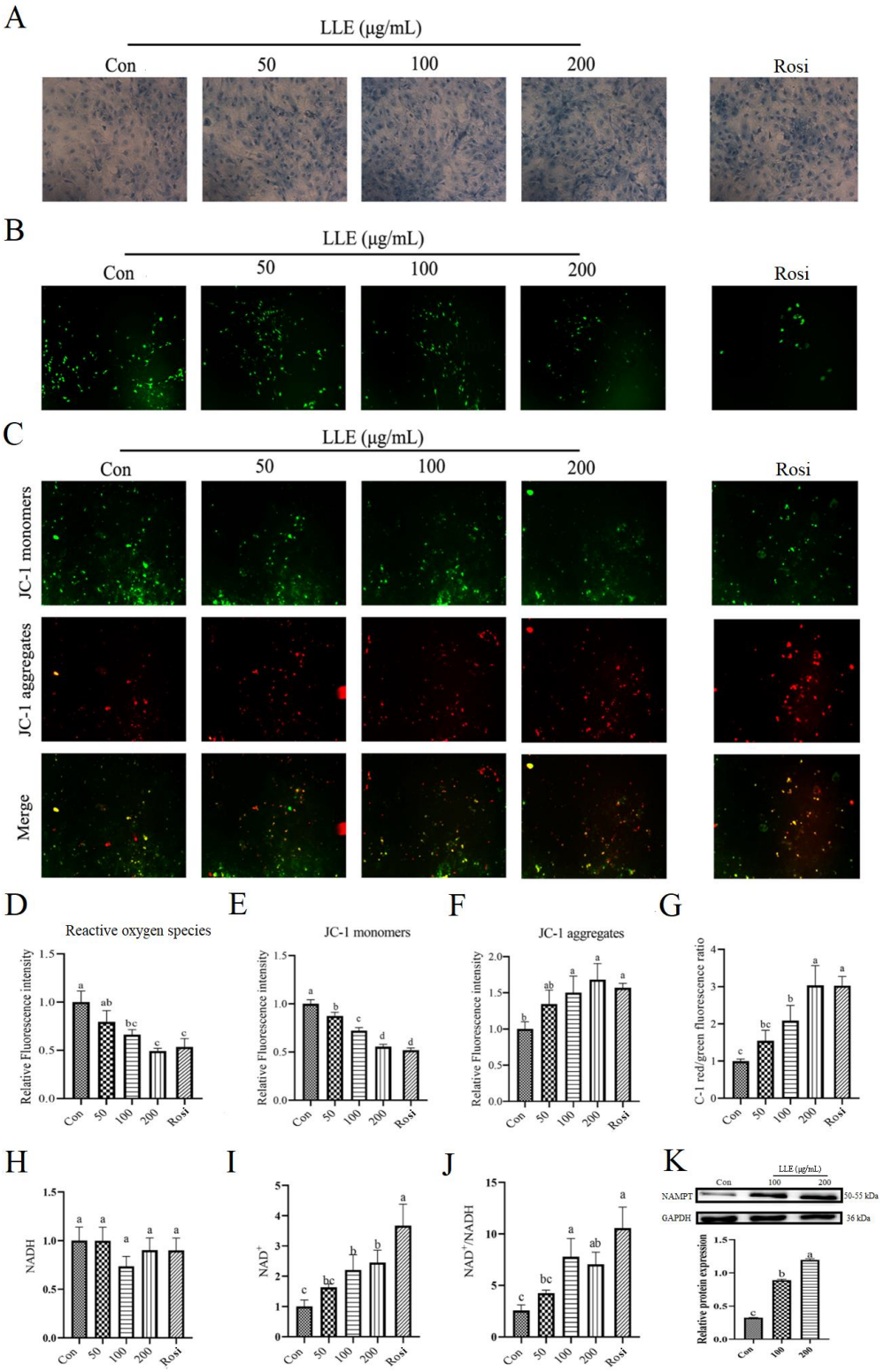
A
LLE (μg/mL)
Con
50
100
200
Rosi
B
LLE (μg/mL)
Con
50
100
200
Rosi
C
LLE (μg/mL)
Con
50
100
200
Rosi
JC-1 monomers
JC-1 aggregates
Merge
D
Reactive oxygen species
Relative Fluorescence intensity
E
JC-1 monomers
Relative Fluorescence intensity
F
JC-1 aggregates
Relative Fluorescence intensity
G
C-1 red/green fluorescence ratio
H
NADH
I
NAD+
J
NAD+/NADH
K
LLE (μg/mL)
Con
100
200
NAMPT
50-55 kDa
GAPDH
36 kDa
Relative protein expression
Con
50
100
200
Rosi

Fig. 2

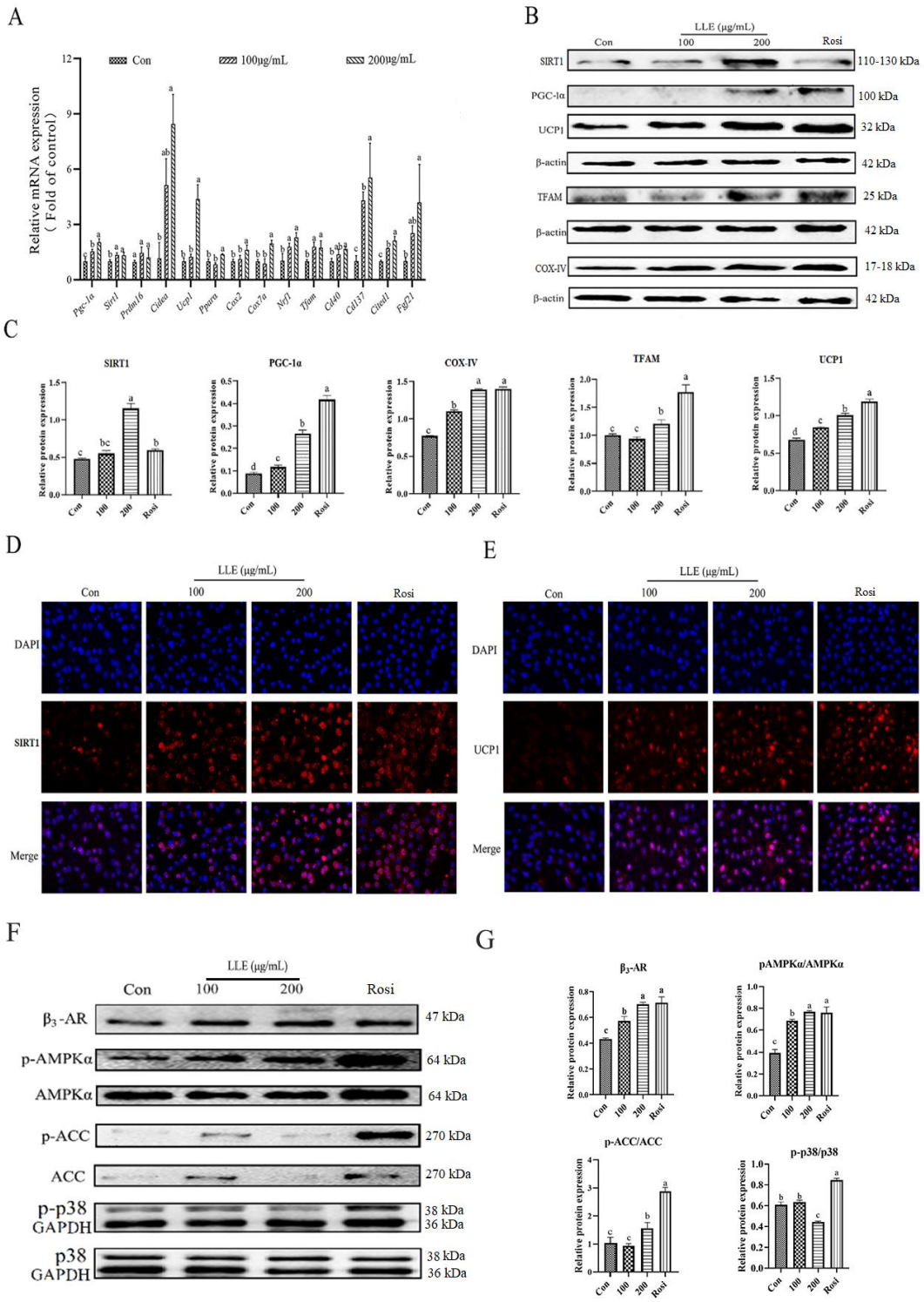
A
Con
100μg/mL
200μg/mL
Relative mRNA expression
(Fold of control)
Pgc-1α
Sirt1
Prdm16
Cidea
Ucp1
Ppara
Cox2
Cox7a
Nrf1
Tfam
Cd40
Cd137
Cited1
Fgf21
B
LLE (μg/mL)
Con
100
200
Rosi
SIRT1
110-130 kDa
PGC-1α
100 kDa
UCP1
32 kDa
β-actin
42 kDa
TFAM
25 kDa
β-actin
42 kDa
COX-IV
17-18 kDa
β-actin
42 kDa
C
SIRT1
PGC-1α
COX-IV
TFAM
UCP1
Relative protein expression
D
LLE (μg/mL)
Con
100
200
Rosi
DAPI
SIRT1
Merge
E
LLE (μg/mL)
Con
100
200
Rosi
DAPI
UCP1
Merge
F
LLE (μg/mL)
Con
100
200
Rosi
β3-AR
47 kDa
p-AMPKα
64 kDa
AMPKα
64 kDa
p-ACC
270 kDa
ACC
270 kDa
p-p38
38 kDa
GAPDH
36 kDa
p38
38 kDa
GAPDH
36 kDa
G
β3-AR
pAMPKα/AMPKα
p-ACC/ACC
p-p38/p38
Relative protein expression

621

622 **Fig. 3**

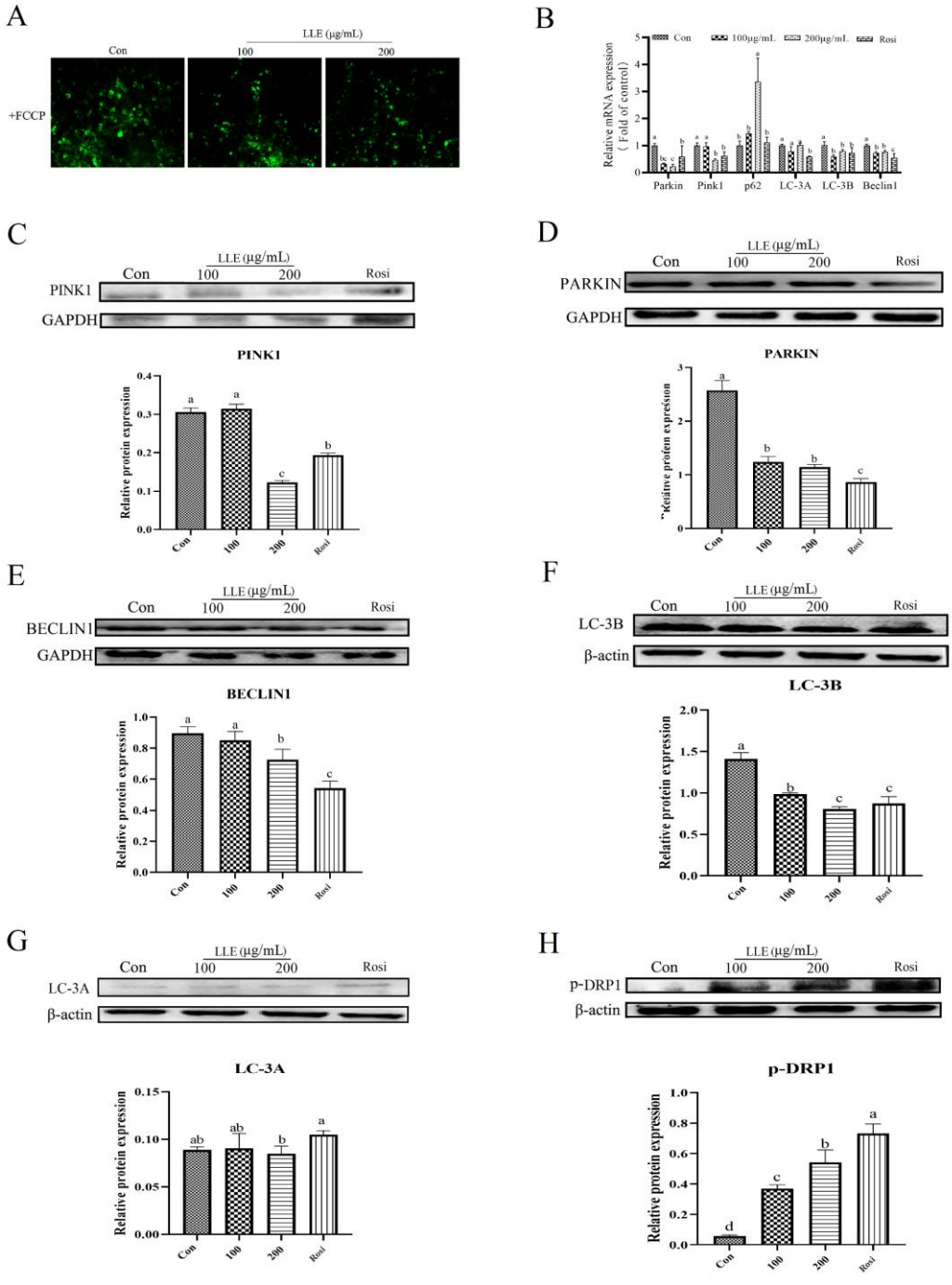
A
LLE (μg/mL)
Con
100
200
+FCCP
B
Con
100μg/mL
200μg/mL
Rosi
Relative mRNA expression
(Fold of control)
Parkin
Pink1
p62
LC-3A
LC-3B
Beclin1
C
LLE (μg/mL)
Con
100
200
Rosi
PINK1
GAPDH
PINK1
Relative protein expression
D
PARKIN
GAPDH
PARKIN
E
BECLIN1
GAPDH
BECLIN1
F
LC-3B
β-actin
LC-3B
G
LC-3A
β-actin
LC-3A
H
p-DRP1
β-actin
p-DRP1

623

624 **Fig. 4**

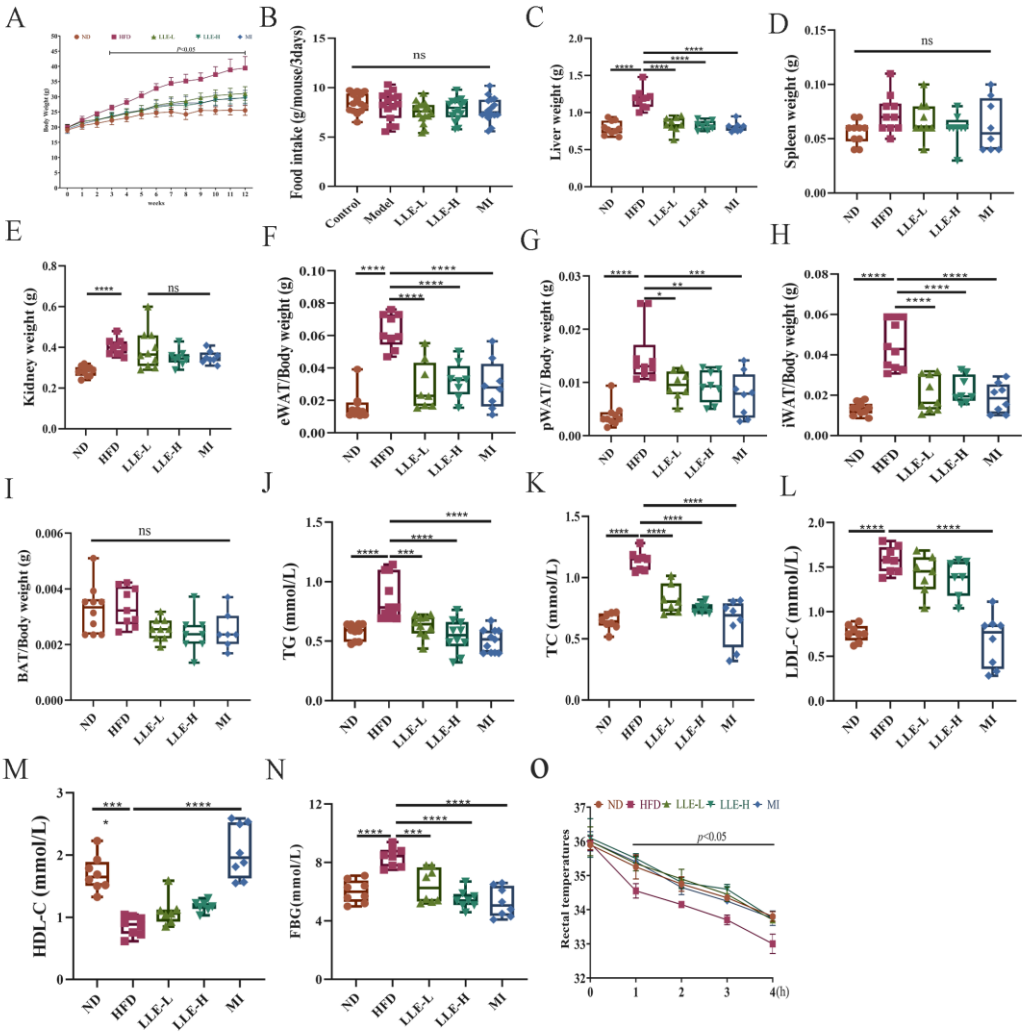
A
B
C
D
E
F
G
H
I
J
K
L
M
N
O
ND
HFD
LLE-L
LLE-H
MI
Control
Model
ns
Food intake (g/mouse/3days)
Liver weight (g)
Spleen weight (g)
Kidney weight (g)
eWAT/Body weight (g)
pWAT/ Body weight (g)
iWAT/Body weight (g)
BAT/Body weight (g)
TG (mmol/L)
TC (mmol/L)
LDL-C (mmol/L)
HDL-C (mmol/L)
FBG(mmol/L)
Rectal temperatures
p<0.05
4(h)

Fig. 5

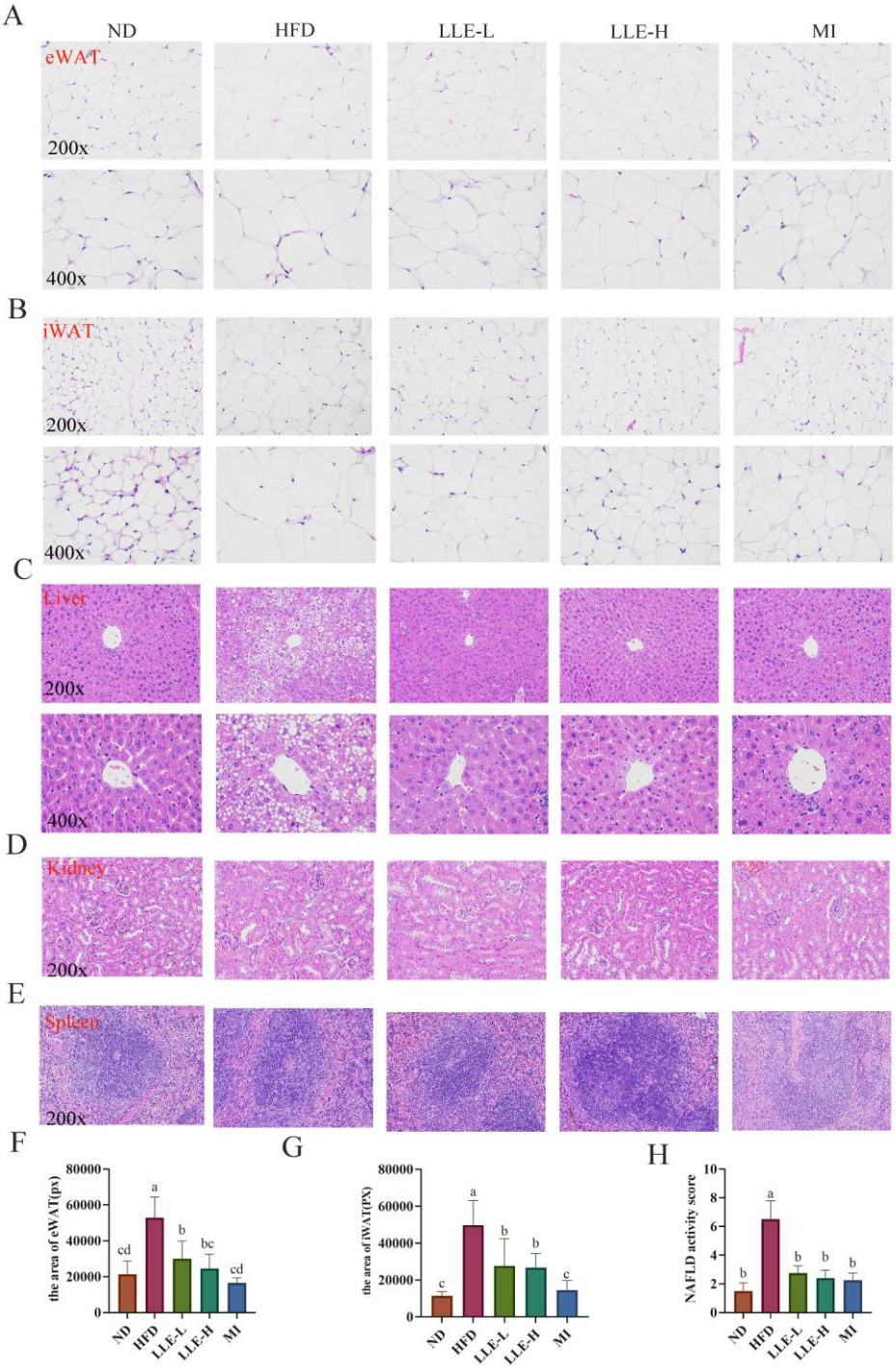
A
ND
HFD
LLE-L
LLE-H
MI
eWAT
200x
400x
B
iWAT
200x
400x
C
Liver
200x
400x
D
Kidney
200x
E
Spleen
200x
F
the area of eWAT(px)
80000
60000
40000
20000
0
a
b
bc
cd
cd
ND
HFD
LLE-L
LLE-H
MI
G
the area of iWAT(PX)
80000
60000
40000
20000
0
a
b
b
c
c
ND
HFD
LLE-L
LLE-H
MI
H
NAFLD activity score
10
8
6
4
2
0
a
b
b
b
b
ND
HFD
LLE-L
LLE-H
MI

Fig. 6

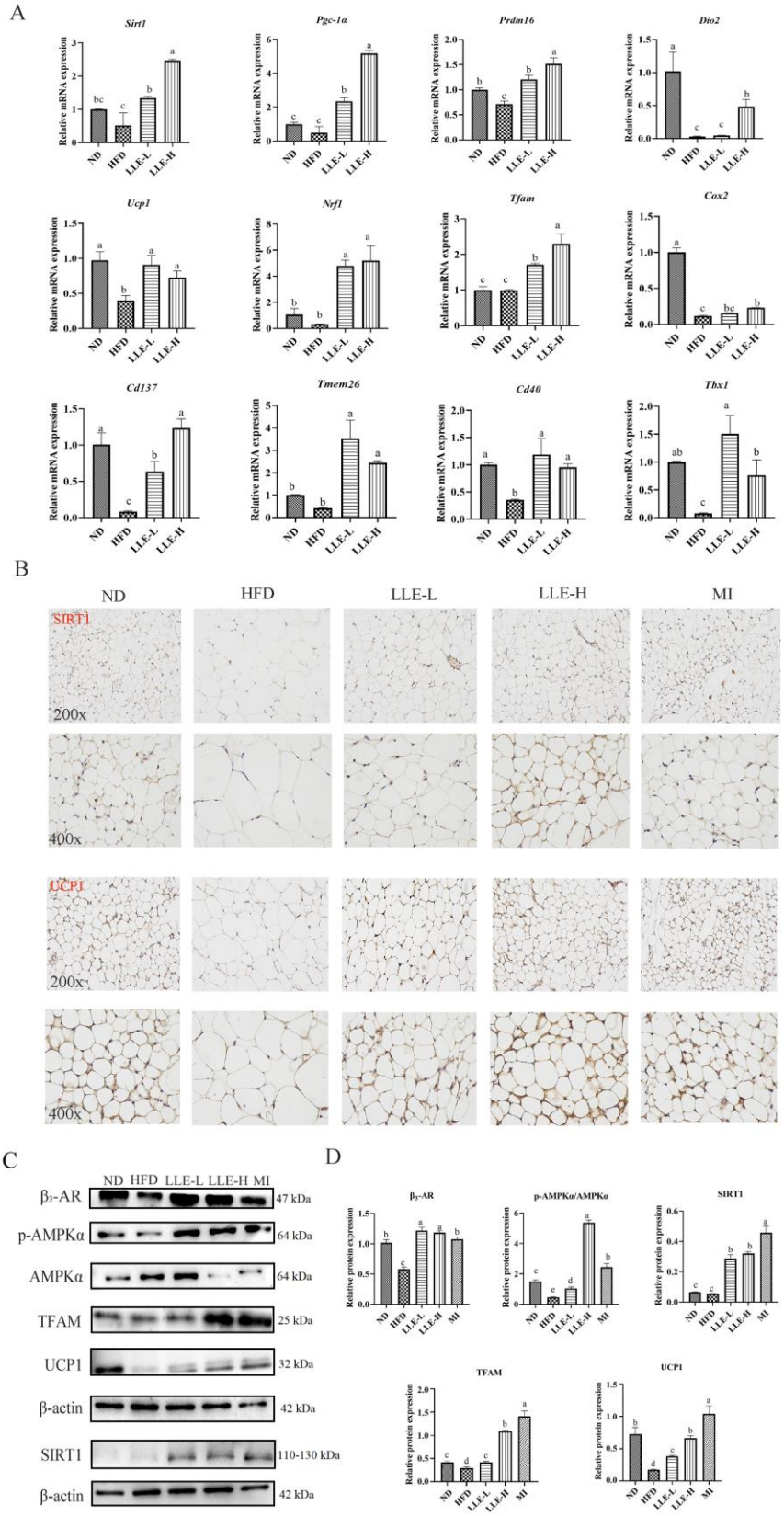
A
Sirt1
Pgc-1α
Prdm16
Dio2
Ucp1
Nrf1
Tfam
Cox2
Cd137
Tmem26
Cd40
Thx1
Relative mRNA expression
ND
HFD
LLE-L
LLE-H
B
ND
HFD
LLE-L
LLE-H
MI
SIRT1
UCP1
200x
400x
C
ND HFD LLE-L LLE-H MI
β3-AR
p-AMPKα
AMPKα
TFAM
UCP1
β-actin
SIRT1
β-actin
47 kDa
64 kDa
64 kDa
25 kDa
32 kDa
42 kDa
110-130 kDa
42 kDa
D
β3-AR
p-AMPKα/AMPKα
SIRT1
TFAM
UCP1
Relative protein expression

Fig. 7

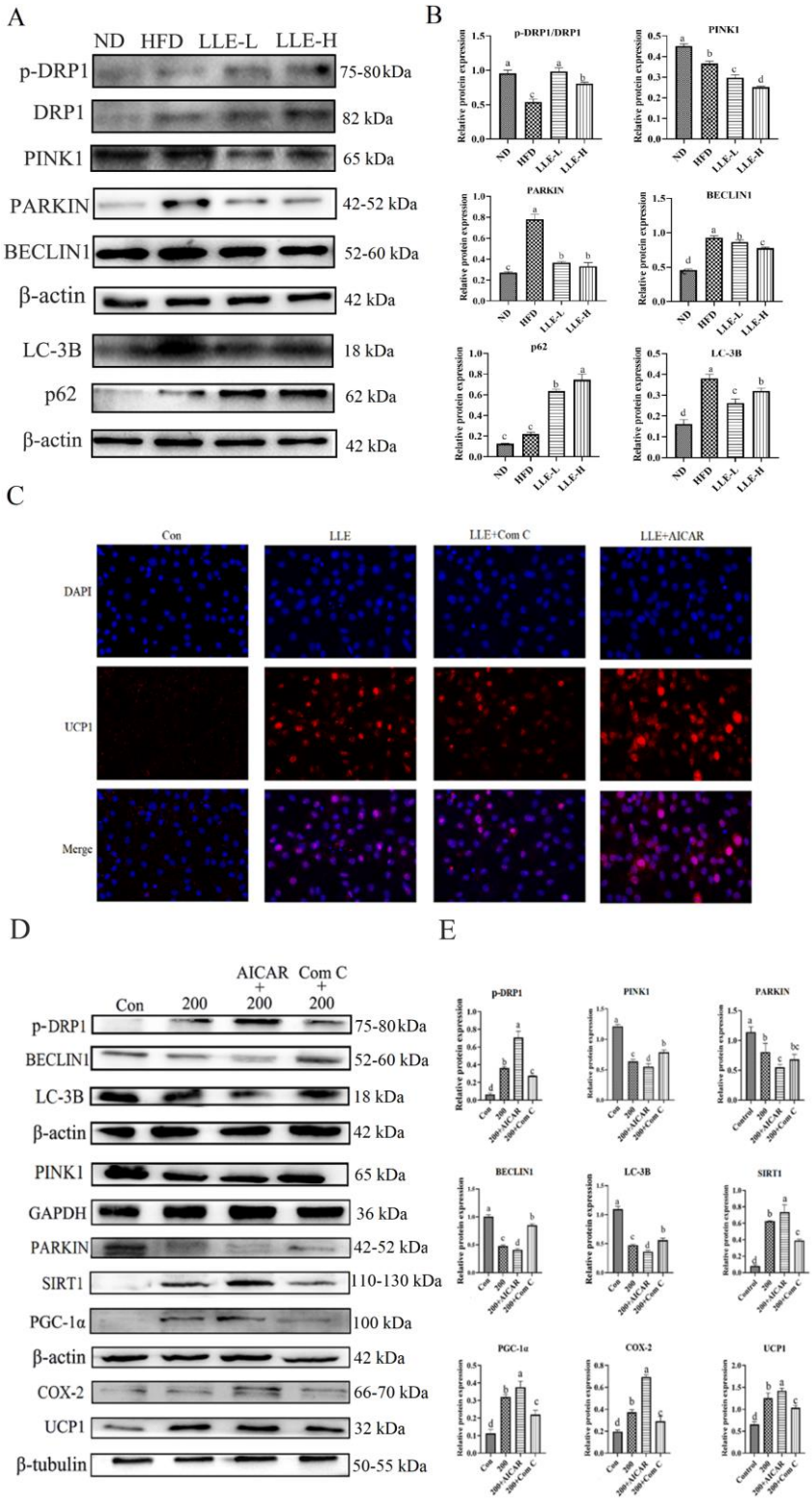

643

644 **Fig. 8**

645

646